Multiple scattering description of intermediate energy deuteron-nucleus elastic scattering

L. Ray
Department of Physics, University of Texas at Austin, Austin, Texas 78712
(Received 22 July 1988)

The nonrelativistic multiple scattering formalism of Watson and Kerman, McManus, and Thaler is applied to the deuteron-nucleus elastic scattering system. An optical potential is constructed to second order in the nucleon-nucleon effective interaction t matrix and is organized in such a way that the usual Watanabe folding potential appears as the leading term. The Watanabe folding potential is constructed by integrating nucleon-nucleus optical potentials evaluated at half the deuteron incident kinetic energy over the deuteron s-state wave function. Corrections to the folding potential are identified which arise from deuteron-nucleon double scattering effects, the deuteron d state, virtual deuteron breakup, additional nuclear medium effects, additional target nucleon correlation effects, and relativistic processes. Many of these corrections do not appear in folding model approaches based on effective, rather than microscopic, deuteron-nucleus Hamiltonians. These additional multiple scattering corrections are second order in the nucleon-nucleon t matrix as is the case for the virtual deuteron breakup process which is often included in numerical calculations. Estimates of several of these additional multiple scattering corrections are provided for 700 MeV deuteron-nucleus elastic scattering. Most are found to be quite small. However, the additional effects of the nuclear medium beyond that already included in the input nucleon-nucleus optical potentials are significant and are comparable in magnitude to the effects of virtual deuteron breakup. It is intended that this multiple scattering approach be applied to deuteron-nucleus elastic scattering at energies of several hundred MeV. Calculations based on this method are presented and compared to recent data for 700 MeV $d+{}^{40}$Ca and ^{58}Ni elastic scattering.

I. INTRODUCTION

Recent, high quality intermediate energy deuteron-nucleus (dA) elastic scattering data[1,2] from the SPES 1 spectrometer facility at the Saturne-2 synchrotron have dramatized the need for theoretical models for the scattering which are appropriate for intermediate energies, which are based on microscopic, many-body approaches to composite projectile-nucleus scattering, and which are readily calculable. The methods that have proven successful throughout the last decade of research in intermediate energy proton-nucleus (pA) scattering are based on multiple scattering theory; either of the nonrelativistic Watson[3] and Kerman, McManus, and Thaler[4] (KMT) types or relativistic Dirac equation generalizations of these.[5-7]

The success of these multiple scattering models stems mainly from the accuracy of the impulse-approximation representation for the effective interaction between the projectile nucleon and the target constituent nucleons at energies of several hundred MeV.[4] The utility of the approach is a result of its rapid convergence with respect to expansions in powers of the effective interaction.[4,8,9] At intermediate energies off-shell dependences,[10] medium modifications,[11] correlations,[9,12-14] and relativistic virtual pair processes[5-7,15] are significant in pA scattering. Presumably such effects are also important in dA scattering. Multiple scattering formalisms provide a straightforward method for including such effects in a rapidly convergent manner.

In the past, studies of dA elastic scattering have been carried out for deuteron energies less than 100 MeV. Numerical analyses of these data are often based on the nonrelativistic folding model approach as presented in the seminal paper by Watanabe.[16] In the simplest version of this model the dA optical potential is obtained by folding proton-nucleus and neutron-nucleus optical potentials evaluated at half the incident deuteron kinetic energy with the deuteron wave function. Such approaches, when augmented with additional tensor potentials,[17-21] provide qualitative descriptions of low energy dA phenomenon.

Numerical improvements to the Watanabe folding model have most often involved calculations of virtual deuteron breakup.[22-27] The dA $(A+2)$-body problem is reduced to a three-body system, consisting of a proton, neutron, and target nucleus. The three-body wave function is expanded in terms of eigenstates of the interacting proton-neutron system; a set of coupled equations is obtained and solved in which the continuum of proton-neutron states is discretized.[22-25] Alternatively, models which utilize the adiabatic approximation are derived for which numerical evaluation is greatly facilitated.[26,27] The calculations indicate significant effects in the dA elastic and reaction channels due to virtual deuteron breakup and general improvement in the description of the data occurs. It is significant, however, that folding model predictions[22] which include virtual breakup corrections still do not adequately explain the recent 700 MeV dA elastic scattering data.

It is important to point out, however, that the theoretical starting point in all of these numerical applications in-

volves an *effective* Hamiltonian for the dA many-body system which depends on nucleon-nucleus elastic scattering optical potentials. Since the folding models are not based on a careful mathematical reduction of the $(A+2)$-body problem a number of intermediate scattering processes are likely to be omitted. For example, double scattering processes involving *both* nucleons in the deuteron with intermediate target nucleus excitation are precluded in these models. It is shown here that the folding model is only accurate to first order in the nucleon-nucleon (NN) effective interaction t matrix; additional multiple scattering terms occur which are second order in the NN t matrix, and are therefore of the same order as the virtual deuteron breakup contribution.

Other, nonrelativistic theoretical approaches for the dA system exist.[28] A cluster expansion formalism with full $(A+2)$-body antisymmetrization has been presented by Kozack and Levin.[28] These authors point out that the full $(A+2)$-body Hamiltonian can be reduced to the effective, folding model Hamiltonian plus three-body correction terms which they discuss. Austern and Richards[28] also point out that nonlocal, three-body operators appear in the full dA Hamiltonian in addition to the usual effective folding model terms. Junkin and Villars[28] presented a formal linked-cluster expansion of the dA optical potential. A three-body model of deuteron-nucleus elastic scattering and stripping reactions using the Faddeev formalism has been developed by Bencze and Doleschall[28] and applied to 10 MeV deuteron induced reactions. Bencze, Polyzou, and Redish[28] obtained effective three-body equations of motion for the dA system using the nonrelativistic many-particle reaction theory of Bencze-Redish-Sloan and determined corrections to dA scattering arising from intermediate nucleon pickup-stripping channels. Antisymmetrization effects and three-body like, virtual target excitation corrections in dA scattering have been studied by Pong and Austern[28] using a nonrelativistic, effective dA Hamiltonian with a modified neutron-proton interaction.

The multiple scattering approach presented here essentially specifies the leading order estimates of these additional, three-body terms in the dA optical potential. The results are given in terms of the NN scattering amplitudes in a clear, physically interpretable fashion which is quite amenable to numerical evaluation. Mukherjee[28] presented a Feshbach type projection operator reduction of the full $(A+2)$-body Hamiltonian and also obtained formal corrections to the folding model potential. The formalism presented here is essentially equivalent to that of Mukherjee. However, the corrections obtained in this previous work were given in terms of the fundamental NN interaction rather than in terms of the effective NN interaction of multiple scattering theory for which convergence of the expansion series is much more rapid.

Formal developments of relativistic models for the dA system have also been presented. Applications of the Bethe-Salpeter, Proca, and Weinberg equations have been formally studied by Santos and collaborators.[29] Calculations for dA observables utilizing a two-particle Dirac Hamiltonian with phenomenological nucleon-nucleus Dirac optical potentials have been applied to 80 MeV $d+{}^{58}$Ni data.[30] A phenomenology based on the relativistic, spin-1 Kemmer-Duffin-Petiau equation has been applied to 400 MeV $d+{}^{58}$Ni data and is being applied to the 700 MeV dA data.[31]

The principal goals of the work presented here are (1) to obtain a formal description of dA elastic scattering using the techniques of multiple scattering theory and (2) to provide numerical calculations of the resulting multiple scattering theory corrections to the lowest order, Watanabe folding potential model. A dA optical potential is derived which is accurate to second order in the NN effective t matrix, and numerical calculations for 700 MeV $d+{}^{40}$Ca and ^{58}Ni elastic scattering differential cross sections and spin observables are presented. The best available pA optical potentials, both theoretical and phenomenological, are used in the lowest-order folding potential. Relativistic virtual pair effects have been included implicitly in the pA optical potentials and explicitly in the nonrelativistic multiple scattering formalism by way of effective, three-body interactions which are treated as perturbations to the dominant two-body effective interaction t matrices. Most of the multiple scattering corrections obtained here are small for the case studied at 700 MeV. However, those due to additional nuclear medium effects and virtual deuteron breakup are significant. These results suggest that folding model calculations which include both the additional nuclear medium effects discussed here and virtual deuteron breakup corrections[22–27] could provide the best theoretical description of the 700 MeV dA data presently available.

In the following section the nonrelativistic multiple scattering formalism is applied to the nucleon-deuteron, nucleon-nucleus, and deuteron-nucleus scattering systems. In Sec. III methods for estimating the multiple scattering corrections are given along with details regarding the calculation of the leading order folding potential. Numerical results for 700 MeV $d+{}^{40}$Ca and ^{58}Ni are presented and discussed in Sec. IV, followed in Sec. V by a summary of these results and some conclusions.

II. MULTIPLE SCATTERING FORMALISM

A. Nucleon-deuteron scattering

It is assumed that the nucleon-deuteron $(N+d)$ scattering system can be described by the three-body, Schrödinger operator equation given by

$$\left[h_{Nd}+H_D+\sum_{i=1}^{2} v_{ij}+\bar{V}_{d;j}\right]|\psi_{N(j),d}\rangle = E_{N(j),d}|\psi_{N(j),d}\rangle \ , \quad (1)$$

where h_{Nd} is the relative $N+d$ center-of-momentum system (c.m.) kinetic energy operator, H_D is the deuteron Hamiltonian, v_{ij} is the two-body interaction, and $\bar{V}_{d;j}$ represents relativistic virtual pair effects in the $N+d$ scattering system which are assumed to be described by an effective three-body interaction. Subscripts (i) and (j) refer to the nucleons in the deuteron and the projectile nucleon, respectively. The wave function for the system is given by $|\psi_{N(j),d}\rangle$. In Eq. (1) and throughout this sec-

tion the projectile nucleon and the target constituent nucleons were assumed to be distinguishable. Use of antisymmetrized projectile nucleon-target nucleon effective interaction t matrices in the final expressions restores projectile-target antisymmetrization to leading order in the two-body effective interaction.[32]

The nucleon-deuteron t matrix is given by

$$T_{dj}=\left[\sum_{i=1}^{2} v_{ij}+\bar{V}_{d;j}\right]+\left[\sum_{i=1}^{2} v_{ij}+\bar{V}_{d;j}\right]G_{Nd}^{(+)}1_D T_{dj} \ , \tag{2a}$$

where

$$G_{Nd}^{(+)}=(E_{N(j),d}-h_{Nd}-H_D+i\varepsilon)^{-1} \tag{2b}$$

and

$$1_D=\sum_{\text{all }\lambda}|\Psi_D^{\lambda}\rangle\langle\Psi_D^{\lambda}| \ , \tag{3}$$

where 1_D projects intermediate $N+d$ scattering states onto the complete set of neutron-proton basis states, $|\Psi_D^{\lambda}\rangle$. The summation in Eq. (3) includes the deuteron ground state along with all continuum states of the neutron-proton system. Explicit dependence on the two-body interaction potential in Eq. (2a) is eliminated by substituting the free nucleon-nucleon scattering t matrix, t_{ij}, given by

$$t_{ij}=v_{ij}+v_{ij}gt_{ij} \ , \tag{4a}$$

where

$$g=(E_{NN}-h_{NN}+i\varepsilon)^{-1} \ . \tag{4b}$$

The quantities E_{NN} and h_{NN} are the assumed NN energy parameter value and kinetic energy operator, respectively. In introducing the two-body t matrix, t_{ij}, it is tacitly understood that the arbitrary two-body energy parameter, E_{NN}, in Eq. (4b) is judiciously chosen so as to minimize matrix elements of the operator quantity $t_{ij}(G_{Nd}^{(+)}1_D-g)t_{ij}$. The choice of Breit frame, two-body kinematics[7,33] for nucleon-nucleus scattering is partly motivated by such considerations. Keeping terms to second order in t_{ij} and lowest order in $\bar{V}_{d;j}$, the following approximate form for the nucleon-deuteron t matrix is obtained:

$$T_{dj}\simeq\sum_{i=1}^{2} t_{ij}+\sum_{i=1}^{2}\sum_{m=1}^{2} t_{ij}G_{Nd}^{(+)}1_D t_{mj} -\sum_{i=1}^{2} t_{ij}gt_{ij}+\bar{V}_{d;j}+\cdots \ . \tag{5a}$$

A simpler form for T_{dj} can be obtained by neglecting the internal, neutron-proton interaction during intermediate scattering states. This further approximation results in the omission of deuteron matrix elements of the operator $t_{ij}(G_{Nd}^{(+)}1_D-g)t_{mj}$. This simplification yields the $N+d$ scattering amplitude evaluated by Alberi, Bleszynski, and Jaroszewicz[33] given by

$$T_{dj}\simeq\sum_{i=1}^{2} t_{ij}+\sum_{\substack{i=1\\ i\neq m}}^{2}\sum_{m=1}^{2} t_{ij}gt_{mj}+\bar{V}_{d;j}+\cdots \ , \tag{5b}$$

where the relativistic correction included in the last term in Eq. (5b) was not discussed in Ref. 33 but was later added in an article by Adams and Bleszynski.[34]

For later use in obtaining the deuteron-nucleus optical potential it is convenient to introduce projection operators P_D^0 and P_D^2 which project the relative $l=0$ and 2 states of the deuteron ground state, respectively, where it is assumed that $P_D\equiv|\Psi_D^{\text{g.s.}}\rangle\langle\Psi_D^{\text{g.s.}}|=P_D^0+P_D^2$. Projecting the nucleon-deuteron t matrix onto initial and final deuteron ground states, the expressions for T_{dj} in Eqs. (5a) and (5b) become

$$P_D T_{dj} P_D=P_D^0\sum_{i=1}^{2} t_{ij}P_D^0+\sum_{i=1}^{2} t_{ij}^{d\text{ state}} +P_D\sum_{i=1}^{2}\sum_{m=1}^{2} t_{ij}G_{Nd}^{(+)}1_D t_{mj}P_D -P_D\sum_{i=1}^{2} t_{ij}gt_{ij}P_D+P_D\bar{V}_{d;j}P_D+\cdots \ , \tag{5c}$$

and

$$P_D T_{dj} P_D=P_D^0\sum_{i=1}^{2} t_{ij}P_D^0+\sum_{i=1}^{2} t_{ij}^{d\text{ state}} +P_D\sum_{\substack{i=1\\ i\neq m}}^{2}\sum_{m=1}^{2} t_{ij}gt_{mj}P_D+P_D\bar{V}_{d;j}P_D+\cdots \ , \tag{5d}$$

respectively, where

$$t_{ij}^{d\text{ state}}\equiv P_D^0 t_{ij}P_D^2+P_D^2 t_{ij}P_D^0+P_D^2 t_{ij}P_D^2 \ . \tag{5e}$$

Deuteron matrix elements of T_{dj} result in 12 independent scattering amplitudes,[33] four of which do not depend on nucleon spin. Of these four amplitudes, one is spin independent, one depends on the component of the deuteron spin-1 vector operator normal to the scattering plane, and two depend on deuteron spin-1 quadrupole or tensor operators. The tensor amplitudes are contained in the single scattering d-state contribution and in the double scattering terms in Eqs. (5c) and (5d). A complete description of the numerical evaluation of the first three terms in Eq. (5d) is given in Ref. 33 in terms of the free NN scattering amplitudes and the deuteron wave function.

B. Nucleon-nucleus scattering

In a similar manner the many-body Schrödinger operator equation for the nucleon-nucleus system can be expressed as

$$\left[h_{NA}+H_A+\sum_{j=1}^{A} v_{ij}+\sum_{\substack{j=1\\ j\neq k}}^{A}\sum_{k=1}^{A}\bar{V}_{i,jk}\right]|\psi_{N(i),A}\rangle =E_{N(i),A}|\psi_{N(i),A}\rangle \ , \tag{6}$$

where h_{NA} is the nucleon-nucleus kinetic energy operator, H_A is the target nucleus Hamiltonian, and the first summation includes all two-body interactions between the ith-projectile nucleon and the jth-target nucleon con-

stituents. The second summation, which hereafter will be referred to as $\bar{V}_3^{(i)}$, represents relativistic virtual pair effects involving the projectile nucleon in intermediate negative energy states between scatterings from two *different* target nucleons (j) and (k).[7,15] As in the previous section, projectile nucleon-target nucleon antisymmetrization will be approximately treated through the use of antisymmetrized NN t matrices.

The nucleon-nucleus t matrix for the ith-projectile nucleon is given by

$$T_{iA}=\left[\sum_{j=1}^{A} v_{ij}+\bar{V}_3^{(i)}\right]+\left[\sum_{j=1}^{A} v_{ij}+\bar{V}_3^{(i)}\right]G_{iA}^{(+)}1_A T_{iA} \ , \tag{7a}$$

where

$$G_{iA}^{(+)}=(E_{N(i),A}-h_{NA}-H_A+i\varepsilon)^{-1} \tag{7b}$$

and

$$1_A=\sum_{\text{all }\lambda}|\Psi_A^{\lambda}\rangle\langle\Psi_A^{\lambda}| \ . \tag{7c}$$

The summation in Eq. (7c) includes all antisymmetric states, $|\Psi_A^{\lambda}\rangle$, of the target nucleus. Convergence of the infinite scattering series is most efficiently achieved through the construction of an optical potential operator, W_i, defined by

$$T_{iA}=W_i+W_i G_{iA}^{(+)}P_0 T_{iA} \ , \tag{8a}$$

where

$$P_0=|\Psi_A^{\text{g.s.}}\rangle\langle\Psi_A^{\text{g.s.}}| \ , \tag{8b}$$

projects the nucleon-nucleus elastic channel in intermediate scattering states. The solution of Eqs. (7a) and (8a) yields an integral equation for W_i in terms of the interactions, v_{ij} and $\bar{V}_3^{(i)}$. Eliminating explicit dependence on v_{ij} by using the free, two-body t matrix in Eq. (4a) yields the following expression for the nucleon-nucleus optical potential operator to second order in t_{ij}. The result is

$$W_i=\sum_{j=1}^{A} t_{ij}+\sum_{j=1}^{A} t_{ij}(G_{iA}^{(+)}Q_0-g)t_{ij} + \sum_{\substack{j=1\\ j\neq k}}^{A}\sum_{k=1}^{A} t_{ij}G_{iA}^{(+)}Q_0 t_{ik}+\bar{V}_3^{(i)}+\cdots \ , \tag{9}$$

where $Q_0=1_A-P_0$ projects intermediate excited nuclear states and the two-body kinematics implicit in t_{ij} are chosen to be that of the Breit kinematic frame.[7]

Matrix elements of the above operator equation, when taken between the ground-state wave function of the nucleus $|\Psi_A^{\text{g.s.}}\rangle$, yield the optical potential function for nucleon-nucleus elastic scattering. The first term corresponds to the so-called "$t\rho$" form or single scattering contribution.[4] The second term accounts for medium modifications to the free NN t matrix arising primarily from Pauli blocking and binding energy effects in the nuclear medium as required by $G_{iA}^{(+)}Q_0$.[11] The third term includes effects due to two-body correlations in the target nucleus[8] while the fourth term is an effective interaction representing relativistic processes.

C. Deuteron-nucleus scattering

The deuteron-nucleus scattering system may now be examined by a straightforward generalization of the derivations presented in the previous subsections. The many-body Schrödinger operator equation for a deuteron projectile is given by

$$\left[h_{dA}+H_D+H_A+\sum_{i=1}^{2}\sum_{j=1}^{A} v_{ij}+\sum_{j=1}^{A}\bar{V}_{d;j}+\sum_{i=1}^{2}\bar{V}_3^{(i)}\right]|\Psi_{dA}\rangle=E_{dA}|\Psi_{dA}\rangle \ , \tag{10}$$

where subscripts (dA) refer to the deuteron-nucleus c.m. system and all other terms in Eq. (10) have been previously introduced.

The dA scattering t matrix, T_{dA}, and optical potential operator, U_{dA}, for elastic scattering are defined by

$$T_{dA}=V_{\text{tot}}+V_{\text{tot}}G_{dA}^{(+)}1_D 1_A T_{dA} \tag{11a}$$

and

$$T_{dA}=U_{dA}+U_{dA}G_{dA}^{+}PT_{dA} \ , \tag{11b}$$

where

$$V_{\text{tot}}=\sum_{i=1}^{2}\sum_{j=1}^{A} v_{ij}+\sum_{j=1}^{A}\bar{V}_{d;j}+\sum_{i=1}^{2}\bar{V}_3^{(i)} \tag{11c}$$

and

$$G_{dA}^{(+)}=(E_{dA}-h_{dA}-H_D-H_A+i\varepsilon)^{-1} \ . \tag{11d}$$

In Eq. (11b), P is defined by

$$P=|\Psi_D^{\text{g.s.}}\rangle\langle\Psi_D^{\text{g.s.}}|\,|\Psi_A^{\text{g.s.}}\rangle\langle\Psi_A^{\text{g.s.}}| \ , \tag{11e}$$

which projects the dA elastic channel.

Solving Eqs. (11a) and (11b) for U_{dA} in terms of V_{tot} and eliminating explicit dependence on v_{ij} using Eq. (4a) yields the formal operator expression for U_{dA}. In carrying out the operator algebra the following projection operators are used:

$$Q_A=|\Psi_D^{\text{g.s.}}\rangle\langle\Psi_D^{\text{g.s.}}|\sum_{\lambda\neq\text{g.s.}}|\Psi_A^{\lambda}\rangle\langle\Psi_A^{\lambda}| \ , \tag{12a}$$

$$Q_D=\sum_{\lambda\neq\text{g.s.}}|\Psi_D^{\lambda}\rangle\langle\Psi_D^{\lambda}|\,|\Psi_A^{\text{g.s.}}\rangle\langle\Psi_A^{\text{g.s.}}| \ , \tag{12b}$$

and

$$Q_{AD}=\sum_{\lambda\neq\text{g.s.}}|\Psi_D^{\lambda}\rangle\langle\Psi_D^{\lambda}|\sum_{\mu\neq\text{g.s.}}|\Psi_A^{\mu}\rangle\langle\Psi_A^{\mu}| \ . \tag{12c}$$

The definition, $Q\equiv Q_A+Q_D+Q_{AD}$, will be used in the

following. Note also that $Q_A+Q_{AD}=Q_0 1_D$. This result is manipulated into a form where the summation over nucleon-nucleus optical potentials, W_i, appears in leading order. The resulting dA optical potential operator is then projected between initial and final deuteron ground states. The final expression for U_{dA}, to second order in the NN t matrix and to first order in the three-body, relativistic effective interactions, becomes

$$
\begin{aligned}
P_D U_{dA} P_D = {} & P_D^0 \sum_{i=1}^{2} W_i P_D^0 + \sum_{j=1}^{A}\sum_{i=1}^{2} t_{ij}^{d\ \text{state}} + P_D \sum_{j=1}^{A}\sum_{i=1}^{2}\sum_{\substack{m=1\\ i\neq m}}^{2} t_{ij} g t_{mj} P_D + P_D \sum_{j=1}^{A} \bar{V}_{d;j} P_D \\
& + P_D \sum_{j=1}^{A}\sum_{k=1}^{A}\sum_{i=1}^{2}\sum_{m=1}^{2} t_{ij} G_{dA}^{(+)} Q_D t_{mk} P_D + P_D \sum_{\substack{j=1\\ j\neq k}}^{A}\sum_{k=1}^{A}\sum_{\substack{i=1\\ i\neq m}}^{2}\sum_{m=1}^{2} t_{ij} G_{dA}^{(+)} (Q_A + Q_{AD}) t_{mk} P_D \\
& + P_D \sum_{j=1}^{A}\sum_{i=1}^{2}\sum_{\substack{m=1\\ i\neq m}}^{2} t_{ij} [G_{dA}^{(+)} 1_D Q_0 - g] t_{mj} P_D + P_D \sum_{\substack{j=1\\ j\neq k}}^{A}\sum_{k=1}^{A}\sum_{i=1}^{2} t_{ij} [G_{dA}^{(+)} 1_D - G_{iA}^{(+)}] Q_0 t_{ik} P_D \\
& + P_D \sum_{j=1}^{A}\sum_{i=1}^{2} t_{ij} [G_{dA}^{(+)} 1_D - G_{iA}^{(+)}] Q_0 t_{ij} P_D \ . \qquad (13)
\end{aligned}
$$

In obtaining this result, very small contributions arising from deuteron d-state corrections to some of the double scattering terms (i.e., those which are second order in t_{ij}) and relativistic terms were ignored.

The energy parameter implicit in t_{ij} through the propagator g, is usually chosen so as to minimize corrections of the form $t_{ij}(G_{dA}^{(+)}Q-g)t_{ij}$. The nucleon-nucleus kinematics implicit in the operator W_i and in the propagator $G_{iA}^{(+)}$ are consequently selected so as to minimize the second term in Eq. (9) given the specification of g. For the calculations presented here the nucleon-nucleus and nucleon-nucleon laboratory kinetic energies were therefore assumed to be one-half that of the deuteron in the dA system as is the usual case in folding model calculations.[16]

The physical significance of the operators in Eq. (13) can be understood in terms of their elastic channel matrix elements. The first term gives rise to the usual Watanabe type folding model in which the proton-nucleus and neutron-nucleus optical potentials are folded with the $l=0$ component of the deuteron wave function. The second term is the lowest order, single scattering correction due to the d-state structure of the deuteron. The third term corresponds to target constituent nucleon double scattering from the two nucleons in the deuteron. The fourth term represents relativistic effects in the target constituent nucleon-deuteron system.[34] The fifth term represents the leading order deuteron breakup correction. Note that for this term, the target nucleus remains in the ground state during intermediate scatterings. The sixth term includes *additional* target nucleus correlation effects which are not contained in the nucleon-nucleus optical potential, W_i. The summations include all pairs of target nucleons and the two combinations of scattering from both nucleons in the deuteron. Note that two distinct processes are accounted for in this term. That proportional to intermediate projection operator Q_A corresponds to pure target nucleus correlation effects where no internal excitation of the projectile deuteron takes place. That containing operator Q_{AD} includes additional virtual deuteron breakup processes which are not accounted for in coupled-channels or adiabatic folding models of deuteron breakup.[22–27] These represent breakup-correlation effects. The next term accounts for *additional* medium modifications which are not included in W_i. The summation includes all processes in which the jth target nucleon is scattered and rescattered by both the neutron and the proton in the deuteron. These latter two terms as well as the breakup contribution are estimated in the following to be among the more important additional multiple scattering corrections to the folding model.

The last two terms in Eq. (13) are correct for the use of nucleon-nucleus optical potentials in the leading order term by requiring deuteron propagation and projection onto physical states of the projectile proton-neutron system during intermediate scattering of the composite deuteron projectile. The first of these corrects the correlation terms included in $(\sum_i W_i)$ while the second [last term in Eq. (13)] corrects the medium modifications contained in $(\sum_i W_i)$. In Eq. (13), matrix elements of the second and third terms contained in $(\sum_i W_i)$ [refer to Eq. (9)] taken between the ground states of the deuteron and nucleus, result in intermediate scattering states in which the target nucleus is elevated into an excited state, the ith nucleon in the deuteron is scattered, and the other nucleon in the deuteron acts as a spectator. Such intermediate states do not completely account for the proton-neutron spectrum which is assumed in the deuteron-nucleus t matrix in Eq. (11a). These last two terms in Eq. (13) should produce only small corrections to the correlation and medium modifications and are therefore neglected.

III. DETAILS OF THE CALCULATIONS AND ESTIMATES OF CORRECTIONS

The deuteron-nucleus elastic scattering optical potential is obtained in coordinate space by forming the ground-state matrix element of the operator expression in Eq. (13) and is given by

$$U^{00}_{dA}(r) \equiv \langle \Psi^{g.s.}_D \Psi^{g.s.}_A | U_{dA} | \Psi^{g.s.}_A \Psi^{g.s.}_D \rangle \ . \quad (14a)$$

For the calculations presented here only the spin-independent, spin-orbit, and Coulomb parts of $U^{00}_{dA}(r)$ are included, where these are given by

$$U^{00}_{dA}(r) \simeq U^{cen}_{dA}(r) + U^{so}_{dA}(r)\mathbf{S}\cdot l + U^{Coul}_{dA}(r) \ , \quad (14b)$$

and $\mathbf{S}$ is the usual spin-1 vector operator.[33]

The first term in Eq. (13) represents the dominant contribution by far. Ideally the nucleon-nucleus potential should be obtained from a theoretical model of the nucleon-nucleus system as described in Sec. II B, and should be one which provides a quantitative description of data at the relevant energies. The cases to be considered here depend on nucleon-nucleus scattering at 350 MeV. At this energy the best theoretical models include the following: (1) the nonrelativistic density dependent G-matrix optical potential of von Geramb;[11] (2) the relativistic one-meson exchange model of Murdock and Horowitz[35] which includes pseudovector pion-nucleon coupling, explicit exchange, and Pauli blocking corrections; and (3) the relativistic, covariant meson exchange model of Tjon and Wallace.[36] Each of these provides qualitative descriptions of the $p+{}^{40}$Ca elastic scattering observables in this energy region. The Dirac phenomenology[37] provides an excellent, quantitative description of these data and produces Schrödinger equivalent central and spin-orbit optical potentials[38] which are similar to those of the above theoretical calculations. Therefore for the $d+{}^{40}$Ca calculations presented here both the Dirac phenomenology and the Murdock and Horowitz potentials were used. Calculations using the former utilize pA optical potentials which accurately fit the 362 MeV $p+{}^{40}$Ca elastic scattering data[39] whereas the results using the latter employ pA potentials which are microscopic in structure.

The analytic form and the parameters of the phenomenological scalar and timelike vector Dirac optical potentials which were fitted to the $p+{}^{40}$Ca, 362 MeV data are given in Table I. For the $d+{}^{58}$Ni 700 MeV calculations the same Dirac potentials were assumed where each radius parameter was scaled by $A^{1/3}$. The same scaling procedure could also be applied to the 700 MeV $d+{}^{16}$O case, however this involves a much larger range of extrapolation for the ^{40}Ca Dirac phenomenology and was not attempted.

TABLE I. Phenomenological Dirac scalar and timelike vector optical potentials for 362 MeV p+^{40}Ca from Ref. 37. The Dirac optical potential is given by $U(r)=U_S(r)+\gamma^0 U_0(r)$, where $U_S(r)$ and $U_0(r)$ are both complex and each part is parametrized by the Woods-Saxon form:

$$V/\{1+\exp[(r-r_0 A^{1/3})/a]\} \ ,$$

where A is the nuclear baryon number. The following parameters were also assumed for ^{58}Ni.

Term	V (MeV)	r_0 (fm)	a (fm)
Real scalar	−419.92	0.9990	0.6681
Imag. scalar	98.98	1.1212	0.5380
Real vector	294.62	1.0066	0.6411
Imag. vector	−97.03	1.1193	0.5516

The Dirac equation with local scalar and timelike vector optical potentials can be reduced to an equivalent second order differential equation which can be solved for the large, "upper" components of the pA four-component Dirac wave function.[38] The solution involves effective, nonlocal potentials. Usually the nonlocal terms are eliminated by a transformation resulting in a second-order Schrödinger-like equation with local, effective potentials, the solution of which yields a scattering wave function which asymptotically approaches that of the upper component of the original Dirac wave function. The equivalent, local potentials also contain Coulomb squared terms[38] which generally have negligible effect and are omitted in this application. The pA optical potentials used in these calculations result in on-shell scattering predictions which are equivalent to that of the Dirac equation except for the small Coulomb squared effects. The off-shell characteristics of these so-called Schrödinger equivalent optical potentials differ from that in the effective, nonlocal potentials in the original second-order reduction of the Dirac equation. Use of either the local or nonlocal effective potentials could result in different predictions for the deuteron-nucleus scattering system. Such effects were not studied here but should be considered in future work.

At these energies the nucleon-nucleus elastic scattering optical potentials are largely isoscalar, hence the neutron-nucleus optical potential was assumed to be equal to the proton-nucleus potential. The contribution to the deuteron-nucleus optical potential was obtained by folding the central and spin-orbit parts of the local, Schrödinger equivalent optical potentials with the $l=0$ component of the deuteron wave function[40] as described in Ref. 16.

The dA optical potential in coordinate space was substituted into the radial Scrhödinger equation with relativistic dA kinematics which is given by

$$\left[\frac{d^2}{dr^2} - \frac{l(l+1)}{r^2} - \frac{2\varepsilon_{dA}}{\hbar^2} U^{00}_{dA,lj}(r) + k^2_{dA}\right] \phi_{lj}(r) = 0 \ . \quad (15)$$

where $\varepsilon_{dA} = E_d E_A/(E_d+E_A)$, E_d and E_A are the total, relativistic energies of the deuteron and target nucleus in the dA c.m. system, respectively, k_{dA} is the dA c.m. wave number, and $U^{00}_{dA,lj}(r)$ is obtained from Eq. (14b) for the (l,j) spin-angle partial wave matrix element. The Coulomb potential is assumed to be that due to a uniform sphere of charge with radii 4.162 and 4.578 fm for $d+{}^{40}$Ca and ^{58}Ni, respectively.

The second and third terms in Eq. (13) were calculated using the nucleon-deuteron scattering model of Alberi *et al.*[33] who explicitly separate the scattering amplitude into contributions from single and double scattering and into terms dependent on only the s state of the deuteron and terms which depend on the d state of the deuteron. The resulting invariant amplitudes were converted into nucleon-deuteron scattering amplitudes in the $N+d$ c.m.

given by $f^{(i)}_{dN\ \text{c.m.}}$; these in turn were converted into $N+d$ scattering t matrices, $t^{(i)}_{dN}|_{dA\ \text{c.m.}}$, evaluated in the dA c.m. frame of reference using relativistic kinematics and the Møller invariant relationship for t matrices.[41] These results are summarized as follows:

$$\frac{f^{(i)}_{dN\ \text{c.m.}}}{k_{dN\ \text{c.m.}}} = F^{(i)}_{dN,\ \text{invariant}}, \quad i=1,2,\ldots,12 \tag{16a}$$

and (see Ref. 4)

$$t^{(i)}_{dN}|_{dA\ \text{c.m.}} = -2\pi(\hbar c)^2 \frac{\varepsilon_d+\varepsilon_N}{E_d E_N} f^{(i)}_{dN\ \text{c.m.}}, \tag{16b}$$

where dN refers to the $N+d$ system. In each of these equations the superscripts (i) represent each of the 12 nucleon-deuteron scattering amplitudes, $k_{dN\ \text{c.m.}}$ is the dN c.m. wave number corresponding to the dA laboratory kinetic energy, $F^{(i)}_{dN,\ \text{invariant}}$ are the 12 invariant amplitudes computed by Alberi *et al.*,[33,42] ε_d (ε_N) and E_d (E_N) are the total energies of the deuteron (nucleon) in the dN c.m. and dA c.m. systems, respectively. The difference between the full calculation of $t^{(i)}_{dN}|_{dA\ \text{c.m.}}$ and that computed assuming single scattering only and no deuteron d state yields the on-shell portion of the two correction terms,

$$\left[\sum_{i=1}^{2} t^{d\ \text{state}}_{ij} + P_D \sum_{\substack{i=1\\ i\neq m}}^{2}\sum_{m=1}^{2} t_{ij} g t_{mj} P_D\right],$$

appearing in Eq. (13). Matrix element operations of this quantity when taken between the nuclear ground-state wave function (for $J^\pi=0^+$, spin-saturated nuclei) reduce the contribution of 12 dN amplitudes to four. The two remaining tensor amplitudes were neglected since these terms are not expected to be very significant at intermediate energies for the observables considered here.[17] The dN spin-independent and spin-orbit t-matrix corrections were assumed to be local, were folded[43] with realistic target nucleus densities,[44] and the resulting central and spin-orbit dA optical potential corrections added to the Watanabe folding potential discussed at the beginning of this section.

Relativistic corrections to the nucleon-deuteron scattering system primarily affect those observables which depend on the nucleon spin.[34] The effects of relativistic dynamics in the deuteron polarization observables mainly appear at fairly large momentum transfers beyond 3–4 fm^{-1}. Relativistic corrections in dN scattering are less important for example, than the double scattering terms in Eq. (5b).[45] Therefore the dN relativistic correction in Eq. (13) is not expected to be significant for dA scattering. Estimates of these effects could readily be added to the present model in a manner similar to that just described for the deuteron d-state and double scattering corrections.

The fifth term in Eq. (13) explicitly accounts for virtual deuteron breakup via the lowest-order nucleon-nucleus ground-state optical potential. A number of calculations of this process are given in the literature where both coupled-channels[22–25] and adiabatic[26,27] models are utilized. The calculations in these references sum over continuum states of the interacting neutron-proton system while the nucleus is required to remain in its ground state, as is the case specific to the Q_D projection operator in the fifth term of Eq. (13). Calculations of this correction are not presented here but have been carried out for 700 MeV $d+{}^{58}$Ni in Ref. 22. Other contributions to dA elastic scattering from virtual deuteron breakup are implicitly included in the elastic channel matrix elements of the nucleon-nucleus optical potentials and in the remaining terms in Eq. (13).

The multiple scattering approach presented here provides a theoretical basis for understanding the virtual deuteron breakup corrections obtained from effective dA Hamiltonians (as opposed to microscopic dA Hamiltonians) and as calculated by many authors, for example those in Ref. 22. Numerical evaluation of the contributions of the fifth term in Eq. (13) can be carried out assuming either a coupled-channels procedure as in Refs. 22–25, an adiabatic approximation as in Refs. 26 and 27, or by way of explicit evaluation of the nonlocal potential term appearing in Eq. (13).

The sixth term in Eq. (13) represents additional target nucleus correlation contributions to dA scattering which are not accounted for in the sum over nucleon-nucleus optical potentials, $\sum_i W_i$. These additional correlation contributions are due to target nucleus excitation—deexcitation via *different* nucleons in the deuteron projectile. Two distinct processes, proportional to projection operators Q_A and Q_{AD}, are represented in this term. Projection operator Q_A requires the deuteron to remain in its ground state while the nucleus is in an excited state whereas Q_{AD} requires both the deuteron and nucleus to be in excited levels [see Eqs. (12a) and (12c)]. The deuteron breakup-target correlation correction proportional to operator Q_{AD} has not been included here nor has it been included in the coupled-channels and adiabatic breakup calculations in Refs. 22–27. It is expected to be comparable to the other correlation effects implicit in $\sum_i W_i$ and in the Q_A portion of the sixth term in Eq. (13).

In order to estimate the Q_A portion of the additional correlation contribution, the correlation potential in the deuteron-nucleus optical potential, given in terms of the $N+d$ effective interaction t matrix by

$$\sum_{j=1}^{A}\sum_{\substack{k=1\\ j\neq k}}^{A} T_{dj} G^{(+)}_{dA} Q_A T_{dk},$$

was considered. This term was estimated using the methods of Refs. 9 and 12–14 along with the $N+d$ on-shell scattering amplitudes of the model of Alberi *et al.*[33] The above expression is analogous to the correlation (third) term in Eq. (9) for the nucleon-nucleus system. The additional dA correlation correction [sixth term in Eq. (13)] is approximately one-half of the full dA correlation potential so evaluated.

To obtain numerical estimates for the dA correlation potential, the calculations of Ref. 9 for the proton-nucleus correlation potential, given in Eqs. (42)–(44), (50), and (56) in Ref. 9, were used where k_N and μc^2 in

these equations of this reference are interpreted as the dA c.m. wave number and reduced total energy. These terms account for correlations due to target nucleon antisymmetrization, short-range NN repulsion, and target center-of-mass constraints. Pauli correlation contributions to the deuteron-nucleus spin-orbit potential were also included. For purposes of these correlation estimates the $N+d$ c.m. amplitudes of Alberi *et al.*[33] were parametrized with Gaussian functions according to [see Eq. (16a)]

$$f_{dN\ \mathrm{c.m.}} = A + iC\mathbf{S}\cdot\hat{n} + \cdots , \tag{17a}$$

where

$$A = \frac{ik_{dN\ \mathrm{c.m.}}\sigma}{4\pi}(1-i\alpha)e^{-Bq^2} , \tag{17b}$$

$$C = \frac{ik_{dN\ \mathrm{c.m.}}\theta}{4\pi}(1-i\alpha_s)e^{-B_s q^2}\frac{q\hbar c}{2Mc^2} , \tag{17c}$$

S is the deuteron spin-1 vector operator, $\hat{n}$ is normal to the $N+d$ scattering plane, and in Eq. (17c) M is the proton mass. The parameters (σ,α,B) and (θ,α_s,B_s) for 700 MeV dA scattering are $\sigma=56.6$ mb, $\alpha=0.345$, $B=0.9$ fm^2, $\theta=-57.1$ mb, $\alpha_s=-5.17$, and $B_s=0.8$ fm^2. These parameters are used directly in applying the equations for the correlation potentials from Ref. 9. The Pauli, short-range NN repulsion, and center-of-mass correlation functions are taken to be the same as in Ref. 9. The same target densities[44] used in the deuteron d-state and $N+d$ double scattering correction estimates were assumed for the correlation estimate. One-half of the resulting dA correlation potential was added to the preceding dA optical potential to represent the contributions from the Q_A portion of the sixth term in Eq. (13).

The seventh term in Eq. (13) represents additional medium modifications to the dA optical potential which are not accounted for in the Watanabe folding potential. It has a structure similar to the nucleon-nucleus medium correction in Eq. (9). In order to estimate this effect the medium modification to the 350 MeV proton-nucleus elastic scattering optical potential was obtained by subtracting the impulse approximation (no medium corrections) pA optical potential[7,9] from that obtained assuming the density dependent effective NN interaction of von Geramb[11] where realistic nuclear densities were assumed.[44] The resulting correction to the pA optical potential was folded with the deuteron s-state wave function and this result added to the previous dA optical potential.

Based on this estimate the additional medium corrections make a significant contribution to the dA elastic scattering observables (see the following section). The potential significance of such effects warrants a careful study of medium corrections in the deuteron-nucleus system and indicates the need for developing a medium modified deuteron-nucleon, density dependent effective interaction analogous to the NN model of von Geramb.[11] The results of calculations and the numerical significance of these additional multiple scattering corrections are discussed in the following section.

IV. RESULTS AND DISCUSSION

The nonrelativistic multiple scattering model was applied to the 700 MeV polarized deuteron elastic scattering data[1] from ^{40}Ca and ^{58}Ni. The lack of 350 MeV $p+^{16}$O elastic scattering data prevents a similar set of calculations from being performed for the 700 MeV $d+^{16}$O data.[2] The application of the multiple scattering approach to deuteron-nucleus scattering at lower energies demands a careful treatment of medium effects in the $N+d$ effective interaction and lies beyond the scope of the present work. This model was, therefore, not applied to the 200 or 400 MeV d+nucleus data.[1,2] The application of the lowest-order Watanabe folding model to $d+^{40}$Ca and ^{58}Ni is described first followed by a description of the effects produced in the 700 MeV $d+^{40}$Ca elastic scattering observables due to the various correction terms in Eq. (13) as discussed in the preceding section.

The predictions of the local, central and spin-orbit Schrödinger equivalent optical potentials for 362 MeV p+^{40}Ca elastic differential cross section and analyzing power data[39] are shown in Fig. 1. The calculation represented by the solid lines incorporated the phenome-

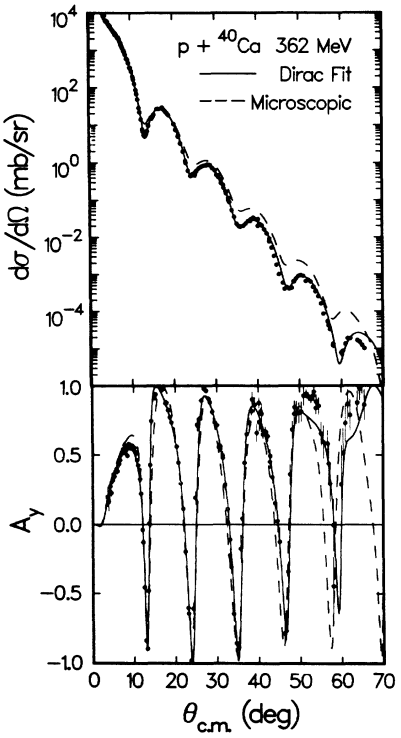

FIG. 1. Experimental data from Ref. 39 and theoretical calculations for 362 MeV p+^{40}Ca elastic scattering differential cross section (upper portion) and analyzing power (lower portion). The curves represent Schrödinger equation calculations using the local, Schrödinger equivalent potentials corresponding to the Dirac phenomenological optical potentials given in Table I (solid curves) and the microscopic, relativistic optical potentials of Ref. 35 (dashed curves).

nological Dirac potentials of Ref. 37, given in Table I, while those indicated by the dashed lines utilized the microscopic, relativistic model of Murdock and Horowitz.[35] The Dirac phenomenology provides an excellent fit to the data. The microscopic prediction of Ref. 35 provides a quantitative description of the analyzing power data and a qualitative representation of the forward angle ($\vartheta \leq 30°$ c.m.) differential cross section data. The overall decline of the microscopic prediction with increasing scattering angle is not quite as rapid as given by the data and the predicted diffraction minima are too shallow relative to the heights of the maxima.

The differences between the Dirac phenomenology and the relativistic, microscopic model descriptions of the $p+{}^{40}$Ca data are reflected in the corresponding Watanabe model predictions for the $d+{}^{40}$Ca, 700 MeV elastic scattering data as shown in Fig. 2. The calculations displayed in this figure utilize just the first term in the dA optical potential in Eq. (13) where the solid and dashed curves correspond to using the local, Schrödinger equivalent nucleon-nucleus optical potentials of the Dirac phenomenology and the relativistic, microscopic model, respectively. Both predictions underestimate the overall magnitude of the differential cross section and the general rate of decrease with increasing scattering angle is too rapid. Results of this quality are typical of those obtained with nonrelativistic Watanabe models,[22] although the results shown here do not underestimate the data as much as in other calculations.[46] The predictions for the vector analyzing power are reasonable while those for the tensor analyzing power, A_{yy}, are only fair.

The Watanabe model predictions for 700 MeV $d+{}^{58}$Ni elastic scattering using the scaled Dirac phenomenological potentials for $p+{}^{40}$Ca are compared with data in Fig. 3. In general the description of the data is similar to that

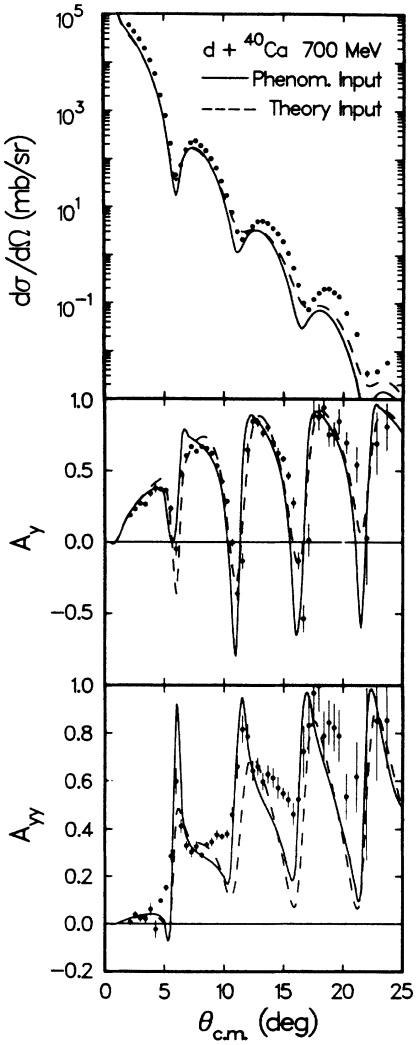

FIG. 2. Experimental data from Ref. 1 and theoretical predictions for 700 MeV $d+{}^{40}$Ca elastic scattering differential cross section (upper portion), vector analyzing power (middle portion), and tensor analyzing power (lower portion). The solid and dashed curves represent Watanabe folding model predictions [using just the first term in Eq. (13)] corresponding to input nucleon-nucleus optical potentials from Dirac phenomenology and microscopic, relativistic theory, respectively.

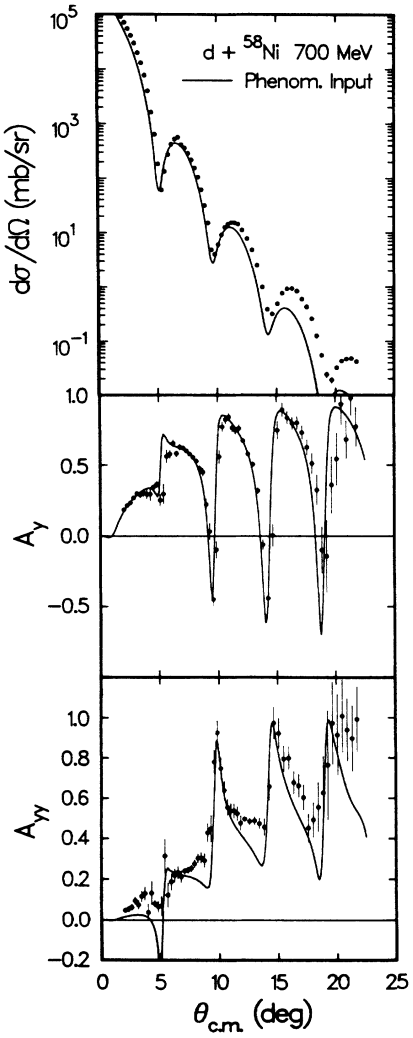

FIG. 3. Same as Fig. 2 except for 700 MeV $d+{}^{58}$Ni elastic scattering. Only the Watanabe folding prediction using the Dirac phenomenological nucleon-nucleus optical potential is shown by the solid curves.

for $d+^{40}$Ca.

Next, the second and third terms in the dA optical potential in Eq. (13) were computed as described in the preceding section and the results added to the Watanabe dA optical potential corresponding to the case for which the Dirac phenomenological pA optical potential was used as input. The effects in the 700 MeV $d+^{40}$Ca elastic scattering observables due to the deuteron d-state and $N+d$ double scattering corrections are separately fairly small and in combination the two effects tend to cancel. The resulting very small changes are shown in Fig. 4 where the solid curves represent the Dirac phenomenology—Watanabe model prediction exactly as shown by the solid curves in Fig. 2 while the dashed curves correspond to calculations including deuteron d-state and $N+d$ double scattering corrections. The combined effects are very small except for A_y and A_{yy} near the minima at larger angles.

The effects in the 700 MeV $d+^{40}$Ca elastic scattering observables due to the additional correlation corrections are shown in Fig. 5. The solid curves represent the Dirac phenomenology—Watanabe model with d-state and double scattering corrections included as discussed in the preceding paragraph (i.e., identical to the dashed curves in Fig. 4). Calculations including the correlation term represented by the sixth term in Eq. (13) (Q_A part only) are indicated by the dashed curves in Fig. 5. Again very small perturbations are found. This result is consistent

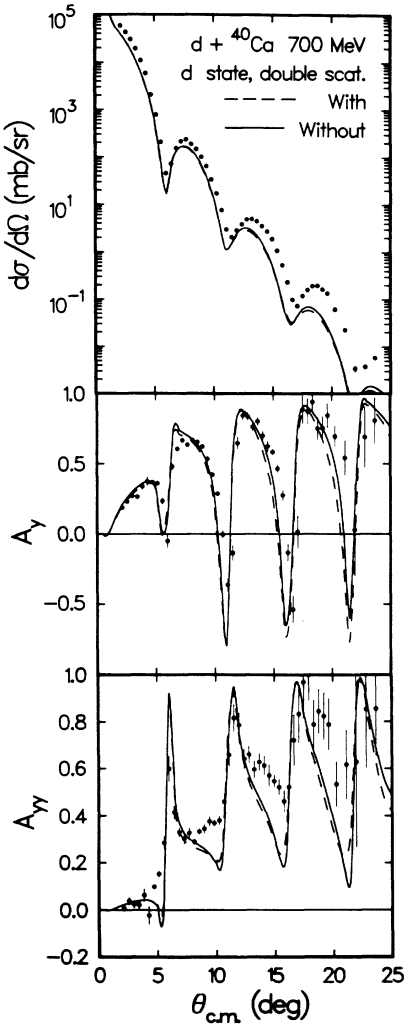

FIG. 4. Effects of deuteron double scattering and d-state corrections [second and third terms in Eq. (13)] for 700 MeV $d+^{40}$Ca based on calculations which use the Dirac phenomenological nucleon-nucleus input potentials. The solid curves represent just the Watanabe folding model prediction and are identical to the solid curves in Fig. 2. The predictions represented by the dashed curves include, in addition, the deuteron double scattering and d-state corrections. The data are from Ref. 1.

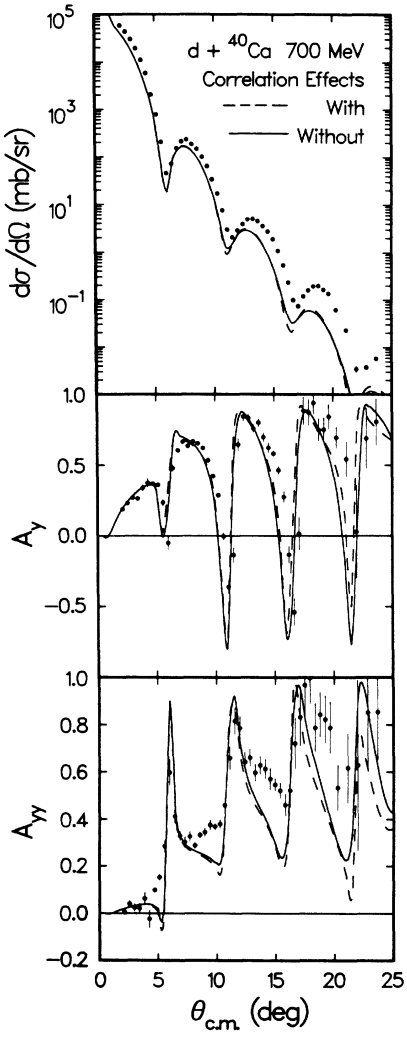

FIG. 5. Effects of additional correlation corrections [Q_A portion of sixth term in Eq. (13)] for 700 MeV $d+^{40}$Ca based on calculations which use the Dirac phenomenological nucleon-nucleus input potentials. The solid curves represent the Watanabe folding model prediction including the deuteron double scattering and d-state corrections and are identical to the dashed curves in Fig. 4. The predictions represented by the dashed curves in this figure include, in addition, the correlation corrections. The data are from Ref. 1.

with calculations of target nucleon correlation effects in the proton plus nucleus system at these energies[47] where the spin-independent, isoscalar NN effective interaction is at a minimum.[48] At higher energies, for example 800 MeV, correlation effects in the pA system are more important, particularly in the spin observables.[49] Therefore effects of this type should be kept in mind whenever higher-energy dA data are being analyzed.

The estimated effects due to additional medium corrections [seventh term in Eq. (13)] are demonstrated in Fig. 6 where significant changes in the 700 MeV $d+^{40}$Ca predictions are seen. The solid curves in Fig. 6 represent the same calculation shown in Fig. 5 by the dashed curves. Calculations including the estimate of the seventh term in Eq. (13) are indicated by the dashed curves. Significant increases in the predicted differential cross sections are produced which move the calculated values toward the data. Significant changes in the structure of the A_y predictions are also noted. These changes in the dA A_y are qualitatively similar to the changes produced in the analyzing power for $p+^{40}$Ca by medium effects.[50] Unfortunately, these additional medium corrections worsen the agreement between experiment and theory. The predictions for A_{yy} are not substantially altered by these additional medium corrections.

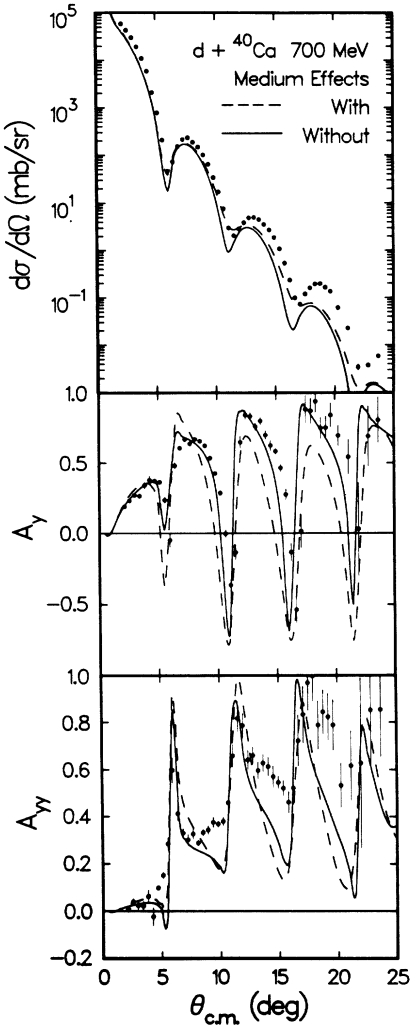

FIG. 6. Effects of additional medium corrections [seventh term in Eq. (13)] for 700 MeV $d+^{40}$Ca based on calculations which use the Dirac phenomenological nucleon-nucleus input potentials. The solid curves represent the Watanabe folding model prediction including the deuteron double scattering and d-state corrections as well as the additional correlation corrections and are identical to the dashed curves in Fig. 5. The predictions represented by the dashed curves in this figure include, in addition, the medium corrections. The data are from Ref. 1.

Corrections for virtual deuteron breakup [fifth term in Eq. (13)], where the target nucleus remains in the ground state, have been calculated for $d+^{58}$Ni at 700 MeV by Yahiro *et al.*[22] using the coupled discretized continuum channels (CDCC) method. These authors show that deuteron breakup processes increase the predicted magnitudes of the differential cross section maxima by significant percentage amounts which become larger as the scattering angle increases. Spin observables A_y and A_{yy} are not significantly affected by breakup processes according to these calculations.

Both of the latter two corrections significantly affect the 700 MeV differential cross section predictions. The additional dA medium corrections have greater impact in the region of the diffractive minima while the effects of the virtual deuteron breakup process are more significant near the maxima. Both perturb the angular distribution predictions by comparable amounts. The virtual deuteron breakup contribution alone, however, is not sufficient to explain the discrepancy between the folding model prediction and the differential cross section data (see Fig. 6 in Ref. 22). Inclusion of the intermediate deuteron breakup process in the 700 MeV $d+^{40}$Ca calculation represented by the dashed curves in Fig. 6 (i.e., the one which includes all the corrections evaluated here) would be expected to yield further improvement in the description of the differential cross section data and provide the best overall theoretical, parameter-free representation of these data currently available.

Finally, note that the virtual deuteron breakup-target nucleus correlation correction [i.e., the Q_{AD} portion of the sixth term in Eq. (13)] has not been calculated and inclusion of this term might result in further perturbations in the dA predictions.

V. SUMMARY AND CONCLUSIONS

In this article, standard, nonrelativistic multiple scattering formalism was applied to intermediate energy deuteron plus nucleus elastic scattering. The utility of this approach to the dA system becomes apparent when the results are compared with those of folding models, such as that originated by Watanabe.[16] Additional physical processes in the dA scattering system were readily elucidated by a straightforward application of a many-body scattering formalism which is based on a fully microscopic Hamiltonian for the $(A+2)$-body system. The additional dynamics, beyond that contained in the simple folding model, which are required to properly describe the dA system have been formally discussed elsewhere.[28] Herein these quantities have been expressed in terms of

effective NN t matrices and put into forms which are readily calculable with standard techniques developed for analysis of proton-nucleus scattering data. The additional terms in the dA optical potential obtained in this work were identified with deuteron-nucleon double scattering, relativistic virtual pair processes in the deuteron-nucleon subsystem, target nucleon correlations, deuteron-nucleon medium modifications, virtual deuteron breakup-target nucleus correlation effects, and projection of intermediate two-nucleon projectile scattering states onto physical neutron-proton basis states. All of these additional terms in the deuteron-nucleus optical potential arise, even if nucleon-nucleus optical potentials are employed in the dA folding model which are very well understood theoretically and which accurately describe nucleon-nucleus scattering data.

Relativistic processes, which are important in proton-nucleus scattering at intermediate energies,[5–7,15,35,36] are also likely to be very significant in multinucleon cluster scattering from nuclei. The relativistic virtual pair process which is evident in proton-nucleus scattering involves three nucleons, in lowest order, and was treated in this nonrelativistic model as an effective, three-body interaction. The relativistic corrections to the dA optical potential were included to leading order.

Generally the additional multiple scattering corrections obtained here are small for the 700 MeV case studied. The additional medium corrections were, however, quite significant. At lower deuteron energies such effects are likely to become even more important while at higher energies the additional correlation corrections could become larger. The effects of virtual deuteron breakup apparently continue to be important at 700 MeV according to the calculations in Ref. 22. However, the virtual deuteron breakup-target correlation correction remains to be calculated and should be studied in future work.

The general success of the multiple scattering approach for the description of intermediate energy nucleon-nucleus scattering (when augmented with relativistic effects) warrants the application of these theoretical techniques to intermediate energy deuteron-nucleus scattering. The results obtained here indicate that nonrelativistic multiple scattering approaches with perturbative relativistic corrections, provide an efficient and satisfactorily convergent model for organizing the complex, many-body scattering problem into a manageable, effective one-body problem which is readily amenable to numerical analysis. Further work along these lines is encouraged.

ACKNOWLEDGMENTS

I would like to thank Dr. B. C. Clark for providing the parameters of the $p+^{40}$Ca Dirac phenomenological potential and for numerous valuable discussions concerning the deuteron-nucleus system. Thanks is also expressed for many helpful discussions with and valuable comments from Dr. R. Kozack and Dr. G. H. Rawitscher. This research was supported in part by the U.S. Department of Energy.

[1]N. Van Sen *et al.*, Phys. Lett. **156B**, 185 (1985).
[2]N. Van Sen *et al.*, Nucl. Phys. **A464**, 717 (1987).
[3]K. M. Watson, Phys. Rev. **89**, 575 (1953).
[4]A. K. Kerman, H. McManus, and R. M. Thaler, Ann. Phys. (N.Y.) **8**, 551 (1959).
[5]J. A. McNeil, J. Shepard, and S. J. Wallace, Phys. Rev. Lett. **50**, 1439 (1983); **50**, 1443 (1983).
[6]B. C. Clark, S. Hama, R. L. Mercer, L. Ray, and B. D. Serot, Phys. Rev. Lett. **50**, 1644 (1983).
[7]L. Ray and G. W. Hoffmann, Phys. Rev. C **31**, 538 (1985).
[8]H. Feshbach, A. Gal, and J. Hüfner, Ann. Phys. (N.Y.) **66**, 20 (1971).
[9]L. Ray, Phys. Rev. C **19**, 1855 (1979).
[10]T. Cheon, Phys. Rev. C **35**, 2225 (1987).
[11]H. V. von Geramb, in *The Interaction Between Medium Energy Nucleons in Nuclei—1982 (Indiana University Cyclotron Facility)*, Proceedings of the Workshop on the Interaction Between Medium Energy Nucleons in Nuclei, AIP Conf. Proc. No. 97, edited by H. O. Meyer (AIP, New York, 1983), p. 44; L. Rikus and H. V. von Geramb, Nucl. Phys. **A426**, 496 (1984).
[12]D. R. Harrington and G. K. Varma, Nucl. Phys. **A306**, 477 (1978).
[13]E. Boridy and H. Feshbach, Ann. Phys. (N.Y.) **109**, 468 (1977).
[14]A. Chaumeaux, V. Layly, and R. Schaeffer, Ann. Phys. (N.Y.) **116**, 247 (1978).
[15]M. V. Hynes, A. Picklesimer, P. C. Tandy, and R. M. Thaler, Phys. Rev. Lett. **52**, 978 (1984).
[16]S. Watanabe, Nucl. Phys. **8**, 484 (1958).
[17]E. J. Stephenson, C. C. Foster, P. Schwandt, and D. A. Goldberg, Nucl. Phys. **A359**, 316 (1981).
[18]R. Frick, H. Clement, G. Graw, P. Schiemenz, and N. Seichert, Phys. Rev. Lett. **44**, 14 (1980).
[19]R. P. Goddard, Nucl. Phys. **A291**, 13 (1977).
[20]P. W. Keaton, Jr. and D. D. Armstrong, Phys. Rev. C **8**, 1692 (1973).
[21]A. P. Stamp, Nucl. Phys. **A159**, 399 (1970).
[22]M. Yahiro, Y. Iseri, H. Kameyama, M. Kamimura, and M. Kawai, Prog. Theor. Phys. Suppl. **89**, 32 (1986); Phys. Lett. B **182**, 135 (1986).
[23]N. Austern, Y. Iseri, M. Kamimura, M. Kawai, G. Rawitscher, and M. Yahiro, Phys. Rep. **154**, 125 (1987).
[24]G. H. Rawitscher and S. N. Mukherjee, Nucl. Phys. **A342**, 90 (1980); G. H. Rawitscher, Phys. Rev. C **9**, 2210 (1974).
[25]E. J. Stephenson *et al.*, Phys. Rev. C **28**, 134 (1983).
[26]R. C. Johnson and P. J. R. Soper, Phys. Rev. C **1**, 976 (1970).
[27]H. Amakawa and N. Austern, Phys. Rev. C **27**, 922 (1983); H. Amakawa and T. Tamura, Phys. Rev. C **26**, 904 (1982).
[28]R. Kozack and F. S. Levin, Phys. Rev. C **33**, 1865 (1986); **34**, 1511 (1986); N. Austern and K. C. Richards, Ann. Phys. (N.Y.) **49**, 309 (1968); W. F. Junkin and F. Villars, *ibid.* **45**, 93 (1967); Gy. Bencze and P. Doleschall, Phys. Lett. **32B**, 539 (1970); Gy. Bencze, W. N. Polyzou, and E. F. Redish, Nucl. Phys. **A390**, 253 (1982); W. S. Pong and N. Austern, Ann. Phys. (N.Y.) **93**, 369 (1975); S. Mukherjee, Nucl. Phys. **A118**,

423 (1968).
[29]F. D. Santos and A. Amorim, Phys. Rev. C **37**, 1183 (1988); F. D. Santos and H. van Dam, *ibid.* **34**, 250 (1986); F. D. Santos, Phys. Lett. B **175**, 110 (1986); F. D. Santos (unpublished).
[30]J. R. Shepard, E. Rost, and D. Murdock, Phys. Rev. Lett. **49**, 14 (1982).
[31]R. E. Kozack, B. C. Clark, S. Hama, V. K. Mishra, G. Kälbermann, R. L. Mercer, and L. Ray, Phys. Rev. C **37**, 2898 (1988).
[32]G. Takeda and K. M. Watson, Phys. Rev. **97**, 1336 (1955).
[33]G. Alberi, M. Bleszynski, and T. Jaroszewicz, Ann. Phys. (N.Y.) **142**, 299 (1982).
[34]D. L. Adams and M. Bleszynski, Phys. Lett. **150B**, 405 (1985). In this work relativistic dynamics are included by using a Dirac propagator in the double scattering term in Eq. (5b).
[35]D. P. Murdock and C. J. Horowitz, Phys. Rev. C **35**, 1442 (1987).
[36]J. A. Tjon and S. J. Wallace, Phys. Rev. C **36**, 1085 (1987); S. J. Wallace, Annu. Rev. Nucl. Part. Sci. **37**, 267 (1987); N. Ottenstein, S. J. Wallace, and J. A. Tjon, University of Maryland Report No. 88-059, 1988; University of Maryland Report No. 88-112, 1988.
[37]E. D. Cooper *et al.*, Phys. Rev. C **36**, 2170 (1987); B. C. Clark, (private communication).
[38]B. C. Clark, in *Medium Energy Nucleon and Antinucleon Scattering,* Vol. 243 of *Lecture Notes in Physics,* edited by H. V. von Geramb (Springer-Verlag, Berlin, 1985), p. 391.
[39]D. Frekers *et al.*, Phys. Rev. C **35**, 2236 (1987).
[40]R. V. Reid, Jr., Ann. Phys. (N.Y.) **50**, 411 (1968).
[41]C. Møller, K. Dan. Vidensk. Selsk. Mat.-Fys. Medd. **23**, 1 (1945).
[42]The deuteron-nucleon scattering amplitudes given in Eq. (4.25) in Ref. 33 were evaluated using the following: (1) the SP87 *NN* amplitudes of R. A. Arndt, J. S. Hyslop III, and L. D. Roper, Phys. Rev. D **35**, 128 (1987); (2) the deuteron wave function of Ref. 40; and (3) the double scattering form factors of Appendix D in Ref. 33 assuming Gaussian parametrizations of the *NN* amplitudes and assuming an average range parameter, $c_{rs}=0.45$ fm^2, in the notation of Ref. 33. The invariant amplitudes, $F^{(i)}_{dN,\text{invariant}}$ in Eq. (16a) are kinematically related to the amplitudes in Eq. (4.25) of Ref. 33 using Eq. (2.11) in Ref. 33.
[43]E. Kujawski and J. P. Vary, Phys. Rev. C **12**, 1271 (1975).
[44]The ^{40}Ca proton density was obtained by unfolding the single-proton electric form factor from the nuclear charge density of I. Sick *et al.*, Phys. Lett. **88B**, 245 (1979). Corrections for the neutron electric form factor were also included as explained in Ref. 9. The neutron density was obtained by adding the difference between the Hartree-Fock-Bogoliubov (HFB) neutron and proton densities to the empirical proton density as discussed in Ref. 7. The HFB densities were those of J. Dechargé and D. Gogny, Phys. Rev. C **21**, 1568 (1980); J. Dechargé, M. Girod, D. Gogny, and B. Grammaticos, Nucl. Phys. **A358**, 203c (1981); J. Dechargé (private communication).
[45]M. Bleszynski *et al.*, Phys. Lett. **106B**, 42 (1981).
[46]H. Kameyama and M. Yahiro, Phys. Lett. B **199**, 21 (1987).
[47]G. W. Hoffmann *et al.*, Phys. Rev. Lett. **47**, 1436 (1981).
[48]W. G. Love and M. A. Franey, Phys. Rev. C **24**, 1073 (1981).
[49]R. W. Fergerson *et al.*, Phys. Rev. C **33**, 239 (1986).
[50]L. Ray, in *The Interaction Between Medium Energy Nucleons in Nuclei—1982 (Indiana University Cyclotron Facility),* Proceedings of the Workshop on the Interaction Between Medium Energy Nucleons in Nuclei, AIP Conf. Proc. No. 97, edited by H. O. Meyer (AIP, New York, 1983), p. 121.